Extending Displacement-Based Earthquake Loss Assessment (DBELA) for the Computation of Fragility Curves

V. Silva, H. Varum
University of Aveiro, Portugal

H. Crowley
EUCENTRE, Pavia, Italy

R. Pinho
University of Pavia, Italy

SUMMARY
This paper presents a new procedure to derive fragility functions for populations of buildings that relies on the displacement-based earthquake loss assessment (DBELA) methodology. In the method proposed herein, thousands of synthetic buildings have been produced considering the probabilistic distribution describing the variability in geometrical and material properties. Then, their nonlinear capacity has been estimated using the DBELA method and their response against a large set of ground motion records has been estimated. Global limit states are used to estimate the distribution of buildings in each damage state for different levels of ground motion, and a regression algorithm is applied to derive fragility functions for each limit state. The proposed methodology is demonstrated for the case of ductile and non-ductile Turkish reinforced concrete frames with masonry infills.

Keywords: seismic risk, loss assessment, fragility functions, DBELA

1. INTRODUCTION

Fragility functions representing the probability of exceeding a set of damage states conditional on a level of ground motion are a fundamental component to describe the physical vulnerability of buildings. The increase in the demand of reliable and more accurate loss estimations has triggered the development of fragility functions based on analytical/mechanical approaches which allow a better representation of the structural behaviour of the building typologies. As discussed by Rossetto and Elnashai (2005), there is not a unique methodology for the development of fragility functions and therefore, each approach will have its limitations and advantages. Several methodologies (Singhal and Kiremidjian, 1996; Dumova-Jovanoska, 2000; Akkar et al., 2005; Erberik, 2008; amongst others) have been proposed with different levels of simplification and efficiency in the past years. However, it is well established that one of the main drawbacks of any analytical methodology is the required computational effort. For this reason, a simplified methodology is proposed in this study. The so-called DBELA methodology (e.g. Crowley *et al*., 2004; Bal *et al*., 2010) is employed to estimate the nonlinear capacity of thousands of RC frames randomly generated and the associated demand from a large set of ground motion records. The fact that several synthetic buildings and ground motion records are used in the calculations allows the consideration of the material and geometrical uncertainties, as well as the record-to-record variability. These calculations are performed within a probabilistic framework and therefore, the parameters that define the fragility functions (i.e. logarithmic mean and logarithmic standard deviation) are also described by a probabilistic distribution, which permits the propagation of the uncertainty in the vulnerability to the risk analysis. This procedure proved to provide a good balance between computational efficiency and reliability, allowing a quick and simple assessment of the physical vulnerability of many different building typologies (e.g. reinforced concrete with frames or shear walls, masonry buildings with concrete or timber slab). This methodology is applied to estimate the statistics of fragility functions for real Turkish reinforced concrete frames with masonry infills.

2. DBELA FRAGILITY FUNCTION CALCULATOR

2.1 Summary of DBELA

The DBELA methodology is a simplified nonlinear static analysis method for the seismic risk assessment of buildings. The method builds upon the urban assessment methodology proposed by Calvi (1999), in which principals of structural mechanics and seismic response of buildings were used to estimate the seismic vulnerability of classes of buildings. Pinho *et al*. (2002) and Glaister and Pinho (2003) carried out further developments on the proposed equations and Crowley *et al*. (2004) adapted the methodology to assess RC buildings and include a probabilistic framework capable of considering the uncertainty on the demand and capacity. In Bal *et al*. (2010) new contributions were added to the methods such as the inclusion of new failure mechanisms and building typologies as well as the evaluation and quantification of the uncertainties of several model parameters.

In this methodology, a randomly generated population of buildings is produced, according to the probabilistic distribution of a set of material and geometrical properties. These distributions are defined based on information gathered from real buildings, as described in Bal *et al*. (2008). Then, the displacement capacity and demand for three limit states needs to be calculated. Each limit state marks the threshold between the levels of damage that a building might withstand, usually manifested by a reduction in its strength or by exceeding certain displacement levels. The displacement capacity is calculated using simple formulae based on the material and geometrical properties of the buildings, and the period of vibration is calculated as a function of the height and ductility. Once these parameters are obtained, the displacement capacity of the first limit state is compared with the respective demand. If the demand exceeds the capacity, the next limit states need to be checked successively, until the demand no longer exceeds the capacity and the building damage state can be defined. If the demand also exceeds the capacity of the last limit state, the building is assumed to have collapsed. Both structural and non-structural vulnerability can be assessed within this method, as long as the appropriate information about each limit state is provided (concrete and steel strain or non structural inter-storey drift corresponding to each limit state). This procedure is schematically depicted in **Figure** 2.1 in which the capacity for each limit state is represented by Δ_i and the associated demand by Sd_i.

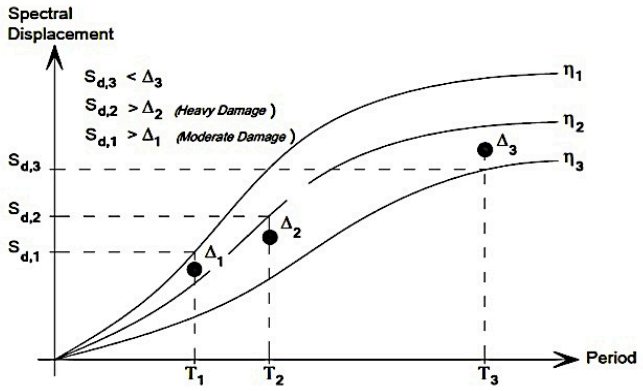

Figure 2.1. Comparison between the capacity for each limit state and the associated demand (Bal *et al*., 2010).

In this example, the demand exceeds the capacity in the first and second limit state but not in the third limit state, thus allocating the building to the third damage state. For the purposes of demonstrating this methodology, four damage states were used (none to slight, moderate, extensive and complete) as defined in Crowley *et al*. (2004). A full description of this methodology, in which the whole procedure is demonstrated step-by-step, can be found in Bal *et al*. (2010).

2.2 Proposed Fragility Methodology

The employment of analytical methods to create fragility functions has been widely used, mainly through the use of capacity spectrum methodologies (e.g. Vacareanu, 2004, Akkar *et al*., 2005,

Rossetto and Elnashai, 2005, Erberik, 2008, amongst others). The methodology that is being proposed herein differs from the aforementioned ones because the method to calculate the nonlinear response of the buildings is simplified and does not suffer from the convergence problems often experienced when using the capacity spectrum method with real accelerograms (e.g. Chopra and Goel, 2000).

This method relies on a Monte Carlo sampler to randomly create populations of buildings, based on a list of random variables of the structural properties defined in the capacity model. A detailed description of the required material and geometric characteristics in the DBELA methodology is presented in Crowley *et al*. (2004). The set of synthetic buildings is then passed to two distinct modules. One that computes the displacement capacity Δ_i based on the material and geometrical properties, and a second one, that calculates the displacement demand Sd_i for each limit state period using over-damped spectra at a level of equivalent viscous damping, representative of the combined elastic damping and hysteretic energy absorbed during the inelastic response, from a set of accelerograms. In order to compute the displacement spectrum from each ground motion record, a module that uses a Newmark integration process (Newmark, 1959) was developed. However, if a user wishes to avoid this additional computational effort, the displacement spectra can also be provided directly as an input to the calculator. The displacement demand for each limit state is then computed by modifying the elastic displacement spectrum by a correction factor η_i, representative of the equivalent viscous damping and limit state ductility. The selection of the set of accelerograms is a key parameter in this methodology and it should comprise a variety of records, respecting the local seismic hazard properties such as magnitude and peak ground acceleration range, most common fault failure mechanism, frequency content, duration or epicentral distance. This use of suites of accelerograms allows the consideration of the effect of the record-to-record variability of the seismic input. Currently there appear to be no formal guidelines for the selection of ground motion records to use in fragility curves generation; focus has been given more to selecting records for assessment and design of single buildings. Many authors choose to gather sets of natural or synthetic records that are subsequently scaled to cover the range of ground motion levels that might occur in the region of interest (e.g. Dumova-Jovanoska, 2000, Singhal and Kiremidjian, 1997). However, this scaling process should not introduce changes in other properties of the records such as the frequency content or event duration, inherent to the magnitude of the event. The wide availability of strong motion databases (e.g.: ITACA [1] (Italy), K-Net/NIED [2] (Japan), ISMN [3] (Iran), GeoNet [4] (New Zealand), Daphne [5] (Turkey), ESD [6] (Europe), PEER [7] (global), COSMOS [8] (global)) should make the task of colleting a large number of natural accelerograms more easily achievable.

Once the capacity and demand displacements for the whole group of synthetic buildings are computed, a module is called to compare both sets of displacements, and thus allocate each building to a certain damage state. Thus, for each ground motion record, percentages of buildings in each damage state can be obtained and fragility curves can be extrapolated (see Figure 2.2). Each ground motion record needs to be represented by an intensity measure level. Within this methodology, it is possible to choose any intensity measure type to represent the record, as long as the necessary information is available. Macroseismic intensities such as MMI or EMS could be a natural choice since there is a direct relationship with the levels of damage in different building typologies. However, keeping track of the intensity at the location where the record was captured is not common and furthermore, macroseismic intensity does not take into account the influence of the frequency content on the structural response. Peak ground motion also shares this last shortcoming and even more importantly, it does not have a clear correlation with damage. The influence of the frequency content on the ground motion can be considered by choosing spectral acceleration or displacement to represent each record (Bommer *et al.*, 2002). Other factors might play an important role in choosing the appropriate intensity measure type such as the availability of accurate GMPE or the possibility of taking advantage of existing seismic hazard data such as USGS ShakeMaps (Allen *et al*., 2008).

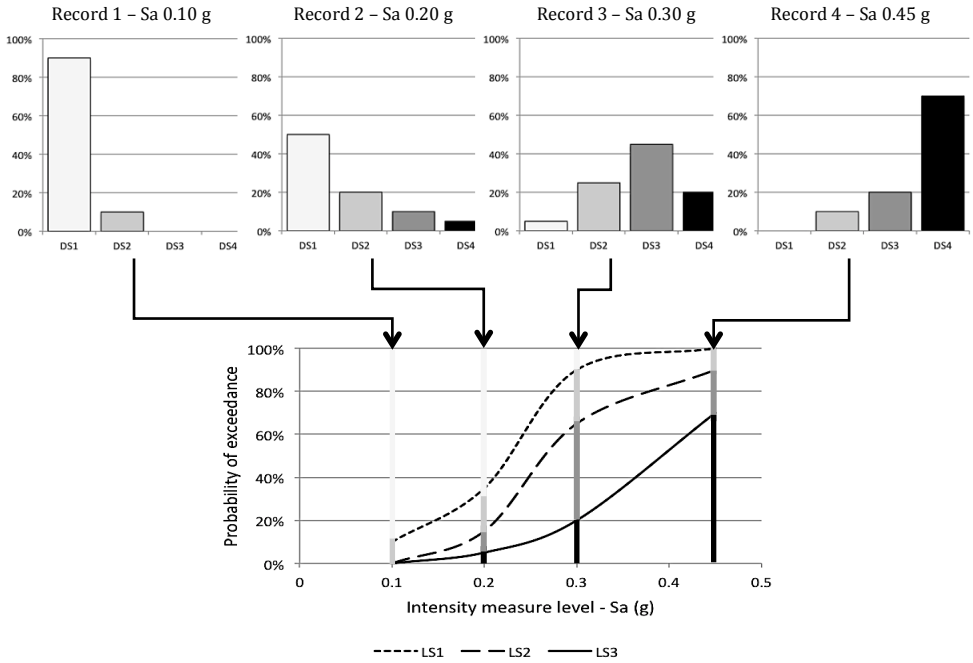

Figure 2.2. Derivation of fragility curves based on building damage distribution.

The fitting of a curve to the list of cumulative percentages versus intensity measure levels is done using the mean least squares method and assuming a lognormal distribution. As showed in the European Syner-G project, where hundreds of fragility curves from the past 30 years were collected (see Crowley *et al*., 2012), this type of distribution is very common to model fragility curves. However, other distributions such as exponential or normal have been used in past vulnerability studies (e.g.: Lang, 2002; Rossetto and Elnashai, 2003) and for this reason, the definition of the probabilistic distribution has not been hard coded, and can easily be modified to other models. The logarithmic mean, λ, and logarithmic standard deviation, ζ, that are estimated for each curve will naturally have some uncertainty associated with them, due to the scatter of the results. Hence, a sampling method was implemented to properly evaluate the uncertainty on the statistics. This method consists in a continuous bootstrap sampling with replacement from the original dataset (Wasserman, 2004). For each dataset that is generated, the associated logarithmic mean and logarithmic standard deviation are estimated. This process is repeated N times, originating N different pairs of logarithmic mean and logarithmic standard deviation, whose distribution can be assumed as normal (Bradley, 2010). From these distributions, confidence intervals for different levels of confidence can be extracted. In Figure 2.3 a curve was fitted to some results and the sampling method was used to derive the distribution of the associated logarithmic mean and logarithmic standard deviation. According to Bradley (2010), 500 synthetic datasets are sufficient to achieve a satisfactory convergence on the results.

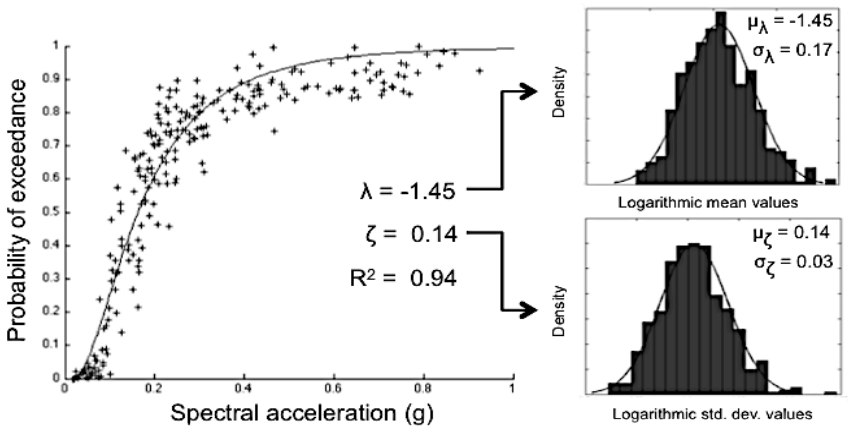

Figure 2.3. Statistical treatment of the parameters of the curve.

The proposed simplified methodology to derive fragility functions using the DBELA methodology is summarized in Figure 2.4.

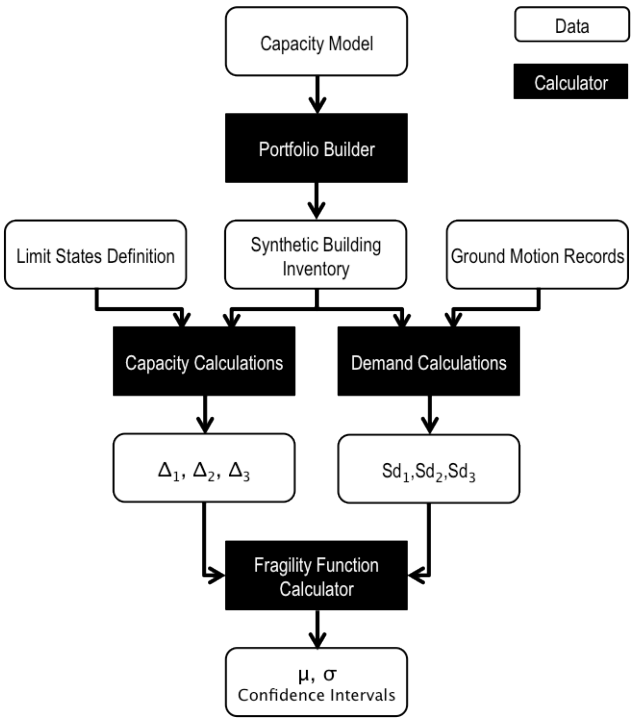

Figure 2.4. Workflow of the DBELA fragility functions calculator.

3. VULNERABILITY FUNCTION CALCULATOR

Fragility functions are commonly converted into vulnerability functions (which provide the distribution of loss, conditional on a level of ground motion), which can then be used in loss assessment. Thus, this framework was also extended to the derivation of these curves. In order to do so, for each intensity measure level a loss ratio needs to be computed, by multiplying the percentage of buildings in each damage state by the associated "damage ratio" (ratio of cost of repair to cost of replacement). The damage ratio per damage state varies significantly according to the building typology (e.g: buildings in California (FEMA, 2003) and Turkey (Bal *et al*., 2008)).

The previously described methodology to derive fragility functions must be applied not only to the mean values of the parameters of each fragility curve, but rather to a set of randomly generated pairs of parameters (logarithmic mean and logarithmic standard deviation per fragility curve), allowing the propagation of this uncertainty to the vulnerability curves. This sampling process needs to be done taking into account the possible correlation between each parameter of the fragility curves. For example, if the correlation coefficient between two parameters is close to 1, then during the sampling process if one of them is sampled to be above the mean, it is likely that the second one will also be sampled with a positive residual. On the other hand, if the pair of parameters has a coefficient of correlation close to 0, then the sampling process is done independently and the way one parameter is sampled does not affect the other one. As previously described, in the bootstrap methodology a list of logarithmic means and a list of logarithmic standard deviations are obtained for each limit state, making a total of six sets of parameters. The correlation coefficients are then computed by analyzing the variation of each set of parameters with respect to the others. An example is presented below to better explain this relation. A set of fragility curves was computed for low-rise Turkish buildings and the bootstrap methodology was used to estimate the probabilistic distribution of the statistics of the three curves. In this process, 100 synthetic datasets were generated and for each dataset, the logarithmic mean and logarithmic standard deviation for each curve were computed. Then, the parameters associated to each dataset were plotted against each other; three of these plots with the

respective correlation coefficient are presented in Figure 3.1.

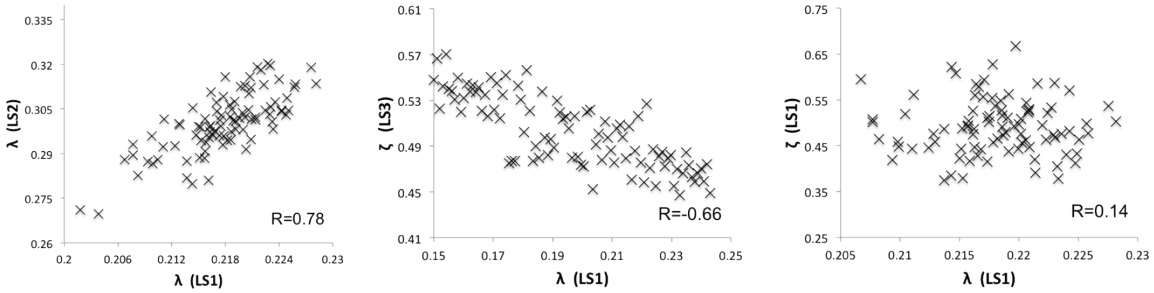

Figure 3.1. Correlation between the distribution parameters of the fragility curves.

The correlation between the parameters can be inferred by analyzing the shape of the scatter. In the first combination, there is a thin dispersion of the data with a positive slope, which means that the values vary relatively linearly and proportionally. In other words, during the bootstrap method every time that a synthetic dataset led to a low mean for the first limit state, it also tended to produce a low mean for the second limit state, and vice-versa. In the second combination there is also a clear correlation between the two parameters but in this case it is negative, which means that the values tend to vary somewhat linearly but inversely. In the last combination, the scatter of the data is characterized by a wide dispersal and therefore, the correlation is not significant.

Different approaches can be followed to randomly sample correlated normal distributions (e.g. Martinez and Martinez, 2002). In this work, a multivariate normal with Cholesky factorization of the covariance matrix approach is followed. This procedure can be described by the following expression:

$$X = ZR + \mu^T \tag{1}$$

Where X represents the resulting n×d matrix with the randomly sampled parameters, Z represents a n×d matrix of standard normal random variable, R is a d×d upper triangular matrix obtained by applying a Cholesky factorization to the covariance matrix, μT stands for a n×d matrix containing the mean of each distribution, n is equal to the number of required samples and d is equal to the number of normal distributions. In this case, d is equal to 6 (a logarithmic mean and a logarithmic standard deviation for each of the three limit state curves) and n should not be lower than 50.

Using the statistics from the previous example and the mean values of the damage ratios proposed by Bal *et al*. (2008), a set of 100 vulnerability curves was calculated. Then, for each intensity measure level, the distribution of the loss ratios was evaluated and a lognormal curve was fit to the data. In Figure 3.2 these results are presented, along with a histogram of the loss ratios and associated lognormal curve for a given spectral acceleration.

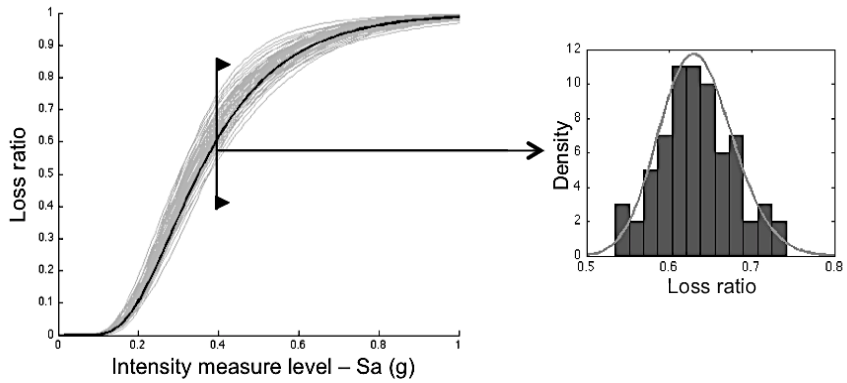

Figure 3.2. Set of vulnerability functions and uncertainty per intensity measure level.

4 CASE STUDY APPLICATION

4.1 Characterization of the RC Building Portfolio

A detailed description of the material and geometric properties of typical reinforced concrete buildings situated in the Marmara region can be found in Bal *et al*. (2008). In this study, hundreds of buildings were used to derive the probabilistic distribution of a list of parameters such as the number of storeys, ground floor and regular height, dimensions of the structural elements, concrete and steel strength, amongst others. To prove that the statistics for each parameter are representative of the population, Bal *et al*. (2008) carried out an exercise in which the number of buildings considered to derive each statistic was continuously reduced, and the respective results were compared with the ones based on the whole sample. It was concluded that even considering a reduced number of buildings, the results were still similar (within a 5% error). The buildings that were legal and designed according to the 1998 Turkish Earthquake Code were treated separately from the ones that were illegal or built before the implementation of the aforementioned design code, allowing the correct estimation of some parameters that are greatly influenced by the code level (e.g. steel and concrete resistance, beam and column width). With regards to the building height, it was necessary to aggregate the buildings into low-rise (1-3 storeys), mid-rise (4-7 storeys) and high-rise (8+ storeys). In Table 4.1, the organization of the building typologies is presented, along with the attributed code and percentage of each building height within each typology.

Table 4.1. Classification of the building typologies in Turkey.

Structure type	Code level	Height	Code	# of storeys	Percentage
RC frames with masonry infills	Low code (non-ductile)	Low-rise	RC-LC-LR	1	17
				2	40
				3	43
		Mid-Rise	RC-LC-MR	4	33
				5	34
				6	22
				7	7
		High rise	RC-LC-HR	8	50
				9	50
	High code (ductile)	Low-rise	RC-HC-LR	1	11
				2	22
				3	67
		Mid-rise	RC-HC-MR	4	49
				5	32
				6	17
				7	2
		High-rise	RC-HC-HR	8	50
				9	50

4.2 Ground Motion Input

For the selection of the accelerograms to be used in the calculations, a study was carried out with the purpose of understanding the seismic properties of the region of interest. According to the work of Kalkan *et al*. (2008), in which a probabilistic seismic hazard analysis for the Marmara region was performed, the following conditions were applied in the selection of the records:

- Range of moment magnitude: 6.0 to 7.4 Mw;
- Rupture mechanism: strike-slip.

It was also decided not to include records that were at a distance lower than 15 km, with the purpose of avoiding the occurrence of near field effects, which would require the application of near-source factors to amplify the short – and intermediate-period spectral ordinates (Bal *et al*., 2010). Another factor that was taken into account was the frequency range supported by each accelerogram. Records that could not provide reliable results for spectral ordinates between 0.05 and 10 seconds were also excluded. About 240 ground motion records were extracted from the PEER database [7]; the variation of PGA of these records is presented in Figure 4.1.

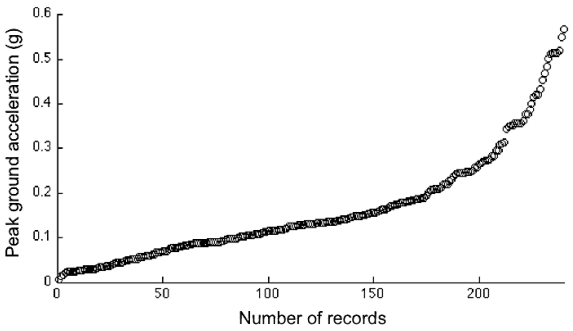

Figure 4.1. Distribution of the PGA values of the selected records.

4.3 Results

Considering the previously defined building typologies, six sets of fragility functions were derived. Although it is widely recognized that spectral ordinates provide a better correlation with damage than peak ground motion (e.g. Shome *et al*. 1998), an exercise was carried out briefly to observe how such correlation varies using the methodology proposed herein. Thus, the correlation between the results and four different intensity measure types was evaluated for each building typology. For low rise, low code RC frames with infill panels, peak ground acceleration, peak ground velocity, spectral acceleration for 0.3 seconds and spectral acceleration for the elastic period were chosen and the average coefficient of correlation for each limit state is presented in Figure 4.2.

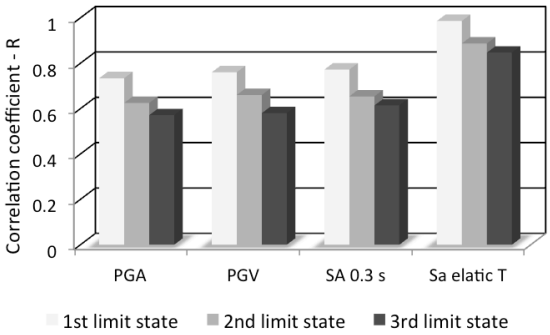

Figure 4.2. Correlation between the results and the set of intensity measure levels for low rise, low code reinforced concrete frames within infill panels.

As expected, there is clearly a stronger correlation between probability of exceedance of the limit state and the spectral ordinates than with peak ground motion. Furthermore, a reduction in the correlation in the second and third limit state is also consistently observed. This decrease is characterized by a larger dispersion of the results, as illustrated in Figure 4.3.

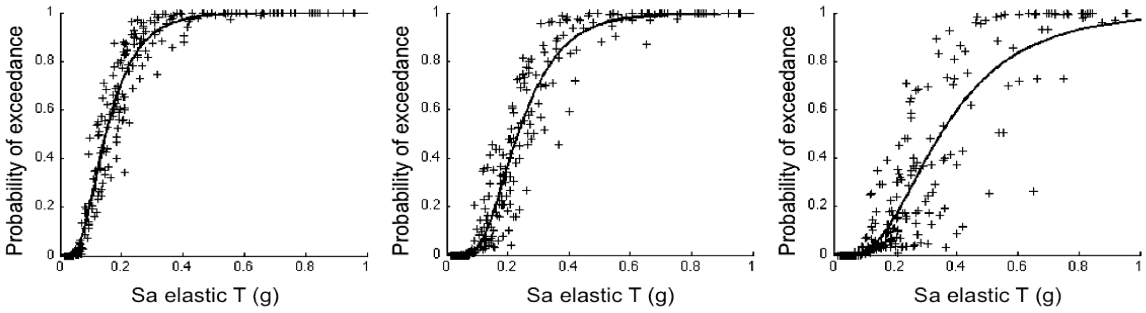

Figure 4.3. Scatter of the results for RC-LC-MR for the first, second and third limit state.

The logarithmic mean and logarithmic standard deviation per limit state for each building typology in terms of spectral acceleration at the elastic period is presented in Table 4.2 and in terms of PGA is

presented in Table 4.3.

Table 4.2. Logarithmic mean and logarithmic standard deviation of each fragility curve in terms of spectral acceleration for the elastic period.

Building typology	T (secs)	LS1			LS2			LS3		
		λ (g)	ζ (g)	R^2	λ (g)	ζ (g)	R^2	λ (g)	ζ (g)	R^2
RC-LC-LR	0.37	-1.262	0.862	0.94	-0.880	0.836	0.80	-0.770	0.846	0.68
RC-LC-MR	0.80	-2.444	0.517	0.95	-1.910	0.551	0.89	-1.716	0.637	0.85
RC-LC-HR	1.34	-3.078	0.492	0.98	-2.453	0.584	0.84	-2.201	0.613	0.76
RC-HC-LR	0.40	-0.967	0.708	0.94	-0.653	0.619	0.78	-0.410	0.663	0.49
RC-HC-MR	0.74	-1.867	0.552	0.96	-1.424	0.484	0.91	-1.023	0.558	0.63
RC-HC-HR	1.33	-2.620	0.479	0.99	-2.110	0.464	0.88	-1.688	0.526	0.62

Table 4.3. Logarithmic mean and logarithmic standard deviation of each fragility curve in terms of peak ground acceleration.

Building typology	LS1			LS2			LS3		
	λ (g)	ζ (g)	R^2	λ (g)	ζ (g)	R^2	λ (g)	ζ (g)	R^2
RC-LC-LR	-1.638	0.591	0.84	-0.956	0.628	0.75	-0.730	0.640	0.70
RC-LC-MR	-2.158	0.817	0.63	-1.212	0.705	0.65	-0.884	0.828	0.59
RC-LC-HR	-2.432	0.892	0.60	-1.240	0.994	0.50	-0.830	1.083	0.48
RC-HC-LR	-1.411	0.624	0.82	-0.749	0.637	0.69	0.012	0.887	0.49
RC-HC-MR	-1.678	0.727	0.65	-0.958	0.675	0.54	-0.011	0.997	0.43
RC-HC-HR	-1.826	0.952	0.58	-0.870	0.926	0.49	0.546	1.456	0.41

5. CONCLUSIONS

In this study a simplified methodology for the derivation of fragility and vulnerability functions based on the DBELA approach was presented. The procedure relies on a probabilistic framework, which allows the consideration of the material and geometric uncertainties of the considered building typology, as well as the variability in the ground motion records. This procedure provided a good balance between computational efficiency and reliability, allowing a quick but accurate assessment of the physical vulnerability. The reliability of this method has been further investigated by Silva *et al*. (2012a), wherein fragility functions for the same building typologies were derived using more robust techniques such as nonlinear static and dynamic analyses, and similar fragility functions were obtained. Due to its modular and flexible architecture, the method presented herein can be applied to any building typology. This framework has been developed as an open source effort and can be found in a repository at GitHub [9]; the fragility and vulnerability models produced with this tool can be directly used in the open source software, OpenQuake, for seismic hazard and risk assessment being developed by the Global Earthquake Model [10] (Silva *et al*., 2012b).

REFERENCES

Allen, T. I., Wald, D. J., Hotovec, A. J., Lin, K., Earle, P. S. and Marano, K. D. (2008). An Atlas of ShakeMaps for selected global earthquakes. U.S. Geological Survey Open-File Report 2008-1236, 47 p.

Akkar, S., Sucuoglu, H., and Yakut, A. (2005) "Displacement-based fragility functions for low- and mid-rise ordinary concrete buildings", *Earthquake Spectra* 21(4), 901-927.

Bal, I. E., Crowley, H. and Pinho, R. (2008) "Displacement-Based Earthquake Loss Assessment for an Earthquake Scenario in Istanbul", *Journal of Earthquake Engineering*, 12: S2, 12 — 22.

Bal. I.E., Crowley, H. and Pinho, R. (2010) "Displacement-based earthquake loss assessment: Method development and application to Turkish building stock," ROSE Research Report 2010/02, IUSS Press, Pavia, Italy.

Bommer, J., Spence, R., Erdik, M., Tabuchi, S., Aydinoglu, N., Booth, E., Re, D. D., and Pterken, D. (2002). "Development of an Earthquake Loss Model for Turkish Catastrophe Insurance". *Journal of Seismology*, 6,

431–446.
Bradley, B.A. (2010) “Epistemic Uncertainties in Component Fragility Functions”. *Earthquake Spectra*, 26(1), 41-62.
Calvi, G. M. (1999). “A displacement-based approach for the vulnerability evaluation of classes of buildings”. Journal of Earthquake Engineering, 26:1091–1112.
Chopra, A. K., and Goel, R. K., (2000). Evaluation of NSP to estimate seismic deformation: SDF systems, Journal of Structural Engineering, 126(4), 482–490.
Crowley, H., Pinho, R., and Bommer, J. (2004). “A probabilistic displacement-based vulnerability assessment procedure for earthquake loss estimation”. *Bulletin of Earthquake Engineering*, 2:173–219.
Crowley, H., Colombi, M., Silva, V. (2012). “Review and collection of fragility functions for European buildings,”.*Proceedings of the 15th World Conference on Earthquake Engineering*, Lisbon, Portugal.
Dumova-Jovanoska, E. (2004). “Fragility Curves for RC Structures in Skopje Region”, *Proceedings of the 13th World Conference on Earthquake Engineering*, Vancouver, Canada, Paper No. 3 (on CD).
Erberik, M., A. (2008) “Fragility-based assessment of typical mid-rise and low-rise RC buildings in Turkey” *Engineering Structures* 30(5), 1360-1374.
Erdik, M. (2007). Discussion of: ‘‘Istanbul at the threshold: an evaluation of the seismic risk in Istanbul,’’ by Pyper Griffiths, J.H., Irfanoglu, A, and Pujol, S., Earthquake Spectra, 23(1), 63–75.
FEMA (2003). “HAZUS-MH Technical Manual” Federal Emergency Management Agency, Washington D.C.
Glaister, S. and Pinho, R. (2003). “Development of a simplified deformation based method for seismic vulnerability assessment”. *Journal of Earthquake Engineering*, 7:107–140.
Lang, K. (2002) Seismic Vulnerability of Existing Buildings, PhD Thesis, Swiss Federal Institute for Technology.
Kalkan, E., Gülkan, P., Yilmaz, N., Celebi, M. (2008) “Probabilistic Seismic Hazard Mapping of the Marmara Region”, Report No. 08-01, Earthquake Engineering Research Center.
Martinez, W. L. and Martinez, A. R. (2002).“Computational statistics handbook with Matlab”. Chapman & Hall/CRC, New York, USA.
Newmark, N.M. (1959) "A method of computation for structural dynamics". *Journal of the Engineering Mechanics Division*, ASCE, Vol. 85, No. EM3, pp. 67-94.
Pinho, R., Bommer, J.J. and Glaister, S. (2002) A simplified approach to displacement-based earthquake loss estimation analysis. In *Proceedings of the 12th European Conference on Earthquake Engineering*, London, England, Paper no. 738.
Rossetto, T. and Elnashai, A. (2003). “Derivation of vulnerability functions for European-type RC structures based on observational data”. *Engineering Structures* 25(10), 1241-1263.
Rossetto, T. and Elnashai, A. (2005) “A new analytical procedure for the derivation of displacement-based vulnerability curves for populations of RC structures”. *Engineering Structures* 27(3), 397-409.
Shome, N., Cornell, C. A., Bazzurro, P., and Carballo, J. E., (1998). Earthquakes, records and nonlinear responses, *Earthquake Spectra* 14, 469-500.
Silva, V., Crowley, H., Pinho, R., Varum, H., Sousa, R., (2012a) “Evaluation of analytical methodologies to derive vulnerability functions,” *Proceedings of the 15th World Conference on Earthquake Engineering*, Lisbon, Portugal.
Silva, V., Crowley, H., Pagani, M., Monelli, D., Pinho, R. (2012b) “Development and application of OpenQuake, an open source software for seismic risk assessment,” *Proceedings of the 15th World Conference on Earthquake Engineering*, Lisbon, Portugal.
Singhal A, Kiremidjian, S. (1997) “A method for earthquake motion–damage relationships with application to reinforced concrete frames”. NCEER report, NCEER-97-0008, SUNY at Buffalo, USA.
Vacareanu, R., Radoi, R., Negulescu, C. and Aldea, A. (2004).“Seismic vulnerability of RC buildings in Bucharest, Romania”. *Proceedings of the 13th World Conference on Earthquake Engineering*, 2004.
Wasserman, L. (2004). “All of Statistics: A Concise Course on Statistical Inference”.Springer, New York, 442pp

Web references
[1] Italian strong motion database ITACA - http://itaca.mi.ingv.it/ItacaNet/
[2] Japan strong motion database - http://www.k-net.bosai.go.jp/
[3] Iran strong Motion Network (ISMN) - http://www.bhrc.ac.ir/ismn/Index.htm
[4] New Zealand strong motion database - http://www.geonet.org.nz/resources/basic-data/strong-motion-data/
[5] Turkish strong motion database - http://daphne.deprem.gov.tr:89/2K/daphne_v4.php
[6] European strong motion database - http://www.isesd.hi.is/
[7] PEER strong motion database - http://peer.berkeley.edu/smcat/
[8] Global strong motion database - http://www.cosmos-eq.org/
[9] Github repository - https://github.com/VSilva/DBELA
[10] Global Earthquake Model – www.globalquakemodel.org